

Prediction of NMR, X-ray and Mössbauer experimental results for amorphous Li-Si alloys using a novel DFTB model

F. Fernandez,^{1,2} M. Otero,^{1,2} M. B. Oviedo,^{3,4} D. E. Barraco,^{1,2} S. A. Paz,^{3,4,*} and E. P. M. Leiva^{3,4}

¹*Universidad Nacional de Córdoba, Facultad de Matemática,*

Astronomía, Física y Computación, Córdoba (X5000HUA), Argentina

²*Consejo Nacional de Investigaciones Científicas y Técnicas (CONICET),*

Instituto de Física Enrique Gaviola, Córdoba (X5000HUA), Argentina

³*Universidad Nacional de Córdoba, Facultad de Ciencias Químicas,*

Departamento de Química Teórica y Computacional, Córdoba (X5000HUA), Argentina

⁴*Consejo Nacional de Investigaciones Científicas y Técnicas (CONICET),*

Instituto de Fisicoquímica de Córdoba (INFIQC), Córdoba (X5000HUA), Argentina

(Dated: May 19, 2023)

Silicon anodes hold great promise for next-generation Li-ion batteries. The main obstacle to exploiting their high performance is the challenge of linking experimental observations to atomic structures due to the amorphous nature of Li-Si alloys. We unveil the atomistic-scale structures of amorphous Li-Si using our recently developed density functional tight-binding model. Our claim is supported by the successful reproduction of experimental X-ray pair distribution functions, NMR and Mössbauer spectra using simple nearest neighbors models. The predicted structures are publicly available.

Global warming caused by fossil fuel burning appears as the biggest environmental problem facing us in this century. One of its major contributions is due to the use of internal combustion vehicles, so a transition to electric vehicles maintaining autonomy and charging time are of vital importance along with habit changes. One of the goals set by the Intergovernmental Panel on Climate Change (IPCC) is to limit the average temperature increase to 1.5°C. This requires changes in technology and human behavior, one of the most important of which is that by 2050, 80% of energy must be supplied by renewable sources [1]. Next-generation lithium batteries are the most promising option to meet the intermittency of renewable energies and power electric vehicles, but they require an increase in their capacity. In this sense, silicon anodes are presented as the best candidate because of the high theoretical capacity of 3579 mAhg⁻¹, which is ten times higher than the current graphite anodes, besides being a cheap, abundant and environmentally friendly material. However, it presents large volumetric changes, of the order of 300%, which lead to structural degradation and a consecutive capacity lost in successive charge/discharge cycles [2].

It has been shown [3] that knowledge at the atomic level of batteries' active materials allow designing strategies that mitigate their limitations and greatly improve performance. This has inspired the scientific community to apply numerous microscopic and spectroscopic characterization techniques. The intrinsic behavior of Si anodes leads to the formation of amorphous Li-Si alloys during charge/discharge that make the short-range structure especially relevant. It has been stated that the crystal-amorphous phase transition occurring for this system represents the main obstacle to improving its electrochemical performance, mainly because it hinders the

attempts to link the atomic structures with the experimental observations [4]. Although there are experiments related to local structures such as nuclear magnetic resonance (NMR), Mössbauer spectroscopy (MB), X-ray pair distribution function (PDF), among others, their interpretation is evasive without a precise theoretical model capable of predicting the microscopic structure of the system and correlate it with the experimental observables. As an example, two different states of Li-ions are always observed, and an intermediate transition that has not yet been elucidated, in voltammograms [5], in diffusion coefficients [6] and in NMR experiments [7].

In previous work, we parametrized a DFTB potential that exhibits a remarkable precision in the prediction of the formation energies for several Li_xSi crystalline and amorphous structures, in a wide range of compositions [8]. Furthermore, using this potential, the simple annealing of crystalline silicon (c-Si) resulted in an amorphous structure (a-Si) with a RDF that is in perfect agreement with experimental results [9]. In light of these results, we show here that the amorphous structures predicted by our model can be used to understand NMR [4, 7, 10, 11], MB [12] and X-ray PDF [13] experimental measurements using a simple nearest-neighbors model.

We started by lithiating the a-Si structure obtained in our previous work [8], following a procedure similar to that proposed by Chevrier and Dahn [14]: (i) Add a Li atom at the center of the largest spherical void, increase the volume and scale coordinates by a factor to obtain the experimental expansion in the system; (ii) Perform an NPT molecular dynamics equilibration for 10ps using the Berendsen Thermostat and Barostat [15] available in the DFTB+ code [16]; repeat these two steps until the desired number of Li atoms is reached. Step (ii)

represents a slight modification that improves the fixed-volume coordinate optimization procedure performed at reference [14]. Following this procedure, we obtain amorphous structures for a wide range of Li_xSi concentrations, from the initial 64 Si atoms ($x = 0$) to a total of 304 for the fully lithiated structure ($x = 3.75$). These obtained structures are available in a public repository [1].

First, we characterize the amorphous structures by computing the partial radial distribution functions (RDF), which describe the probability of finding an atom in a shell at a distance r from a reference atom. As can be seen in Figure S1 of Supplemental Material, the nature of the obtained distributions is typical for amorphous structures, having a definite first peak at short r and decreasing following ones for increasing r . The most interesting behavior to analyze is found in the Si-Si RDF. As lithium concentration increases there is clearly a decrease in the first neighbor peak together with a shift in the second neighbor peak towards larger distances ($3.8 \text{ \AA} \rightarrow 4.7 \text{ \AA}$). This tells us that the Si-Si bonds are being broken during the lithiation and isolated Si appears. It is worth mentioning that the DFTB model used in this work allows to capture these fine chemical features at a low computational cost, showing a great detail in the representation of the electronic structure of many atoms.

Combining the previous partial RDFs allowed us to calculate the total $G(r)$ for each structure, as detailed in the Supplemental Material. The $G(r)$ can be directly compared with the PDF obtained from X-ray measurements [17]. The standing triangles of Figure 1 show the X-ray PDFs for the two extreme cases of unlithiated a-Si (bottom) and full lithiated silicon anode (top), as measured by Laaziri *et al.* [9] and Key *et al.* [4], respectively. For comparison, we include in the same figure the $G(r)$ computed using the following procedures. For a-Si, we directly take the $G(r)$ as an average from our a-Si modeled structures, resulting in an excellent agreement with the experimental measurement, as can be seen at the bottom of the figure. For the case of the fully lithiated silicon anode, the experimental sample is expected to be mainly composed of amorphous $\text{Li}_{15}\text{Si}_4$, although a crystalline contribution to the X-ray PDF may also be expected. In addition, another contribution from pure Si is also possible, mainly due to an incomplete lithiation resulting from various experimental factors such as bad connectivity, kinetically limited events, or even a possible $\text{Li}_{15}\text{Si}_4$ decomposition [4, 7]. Therefore, we have fitted the experimental data shown in figure 1 using a linear combination of the $G(r)$ obtained from the a- $\text{Li}_{15}\text{Si}_4$ and a-Si modeled structures, but also including the crystalline ones (see Supplemental Material). Strikingly, the resulting weights for the crystal phases are quite small, representing only a 9.78% for c- $\text{Li}_{15}\text{Si}_4$ and exactly 0% for c-Si. This highlights the importance of counting with amorphous atomic structures to understand the experimental measurements. On the contrary, a very poor fit

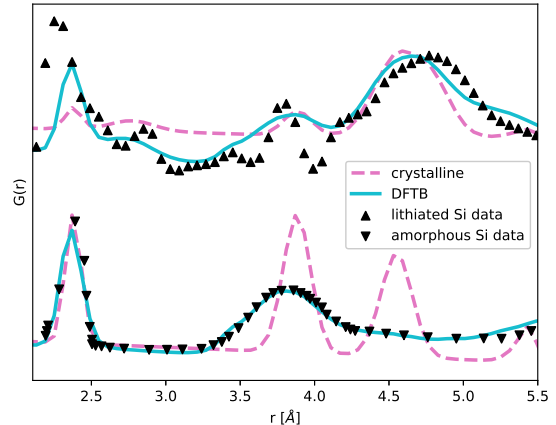


FIG. 1. Pair distribution functions $G(r)$ for amorphous and full lithiated Si contrasted with experimental data. The triangles pointing down correspond to Laaziri’s a-Si experiment [9], while those pointing up correspond to Key *et al.*’s experiment [4].

is obtained if only crystal structures are used, as can be seen at the top of figure 1 (pink curve).

Direct measurement of local atomic structure is challenging, however, some spectroscopic techniques allow us to infer the local structure due to a high dependence of the measured property on the atomic local environment. This is the case for NMR and MB spectroscopy. In previous work, Key *et al.* [7] prepared different Li-Si structures and measured their ^7Li NMR chemical shift spectra. The NMR signal is characterized by a Voigt peak (V), which corresponds to the combination of a Lorentzian that is intrinsic to the NMR phenomena and a Gaussian due to the detector [18]. Each particular nucleus introduces a shift on this signal, the chemical shift, that depends on the electromagnetic shielding caused by the local environment, and therefore the local structure. The total spectra obtained for each sample are the sum of the signal contributions coming from all the ^7Li in the structure. In this spectra, Key *et al.* [7] assigned a peak at 18 ppm to the chemical shift of a ^7Li atom which is near a bonded Si atom. On the other hand, a peak at 6 ppm was attributed to ^7Li near an isolated Si atom. However, it is not clear how to interpret the occurrence of peaks between 6 and 18 ppm, which are in fact observed in the NMR measurements. We propose here a simple nearest-neighbor model to emulate and interpret these features in the NMR spectra. We define a peak position in the spectra including an average of the contributions stemming from all Si atoms sitting in the first coordination shell of a given Li atom as follows:

$$\delta_{Li} = \frac{1}{N_{Si}} \sum_{Si \in \text{NN}} \delta_{\text{Key}}, \quad (1)$$

where δ_{Li} is the chemical shift contribution of the Li atom in question to the global spectra, the sum is considered over all first nearest neighbours (NN) Si atoms (N_{Si}) and δ_{Key} is the shift proposed by Key *et al.* [7], as discussed above. Then, the total chemical shift spectrum has an intensity (I) that results from a sum of Voigt peaks (V) over all the Li atoms in the structure S ,

$$I = \sum_{Li \in S} V(\text{ppm}, \delta_{Li}, \sigma, \gamma), \quad (2)$$

where ppm is the chemical shift, σ and γ are the standard deviations and the half-width at half-maximum of gaussian and lorentzian components, respectively. Finally, an average was taken over all snapshots of our molecular dynamics trajectories.

As a first test of this model, we present the ^7Li chemical shift spectra for the crystalline structures in Figure 2, as calculated from the present assumptions. The atomic configurations were obtained from the Materials Project [19] and the peak width was fitted to the accuracy of the Key *et al.* experiment [7] once the nearest-neighbors model determined the center of the peak. The model presented here corresponds to the continuous lines, while Key's measurements correspond to the points. For all four alloys, the center of the peak is reproduced with high accuracy. In the $\text{Li}_{12}\text{Si}_7$ and Li_7Si_3 alloys, the Si atoms are all bonded. The first forms pentagons of 5 atoms or stars of 4, while in the second one, all the bonds are dumbbells. This shows that in this nearest-neighbors model, all the Li atoms contributions are centered at 18 ppm. In the fully lithiated alloy $\text{Li}_{15}\text{Si}_4$ there are only isolated Si atoms, so all the contributions are centered at 6 ppm. Meanwhile, for $\text{Li}_{13}\text{Si}_4$, isolated Si coexists with dumbbells, making intermediate contributions to the spectra, consistent with experiment.

Having obtained these promising results for the crystalline structures, we now focus on amorphous structures, which are usually found in electrochemical experiments. We calculate the ^7Li chemical shift spectra for different amorphous Li-Si alloys with the proposed nearest-neighbors model using the structures obtained from our molecular dynamics simulation. We considered those structures with x values in Li_xSi that can be related to the voltages used by Key *et al.* [7] to collect the NMR spectra. To facilitate the comparison with our model we have included a peak at -0.3 ppm, which represents the SEI contribution, as suggested by the cited authors. The results are shown in Figure 3 which, apart from some differences explained below, shows an excellent agreement between the computational and experimental results. This is particularly true in the case of the peak at 18 ppm, where the modeling is able to mimic the shift of the peak to 6 ppm at high concentration. This change is the clearest evidence to support the current atomistic view of the system. At the beginning of the lithiation, the configurations contain mainly bonded Si atoms. Then

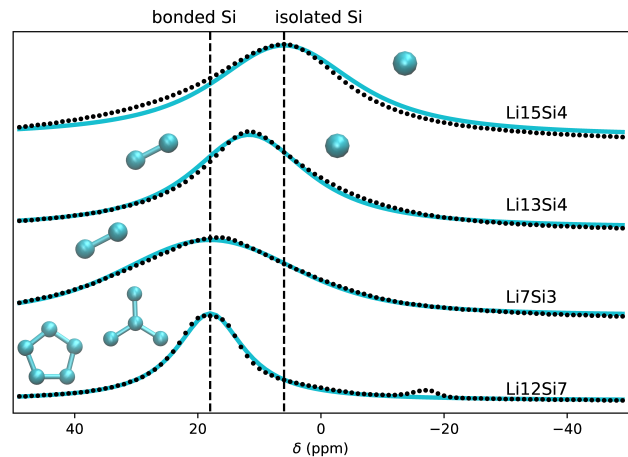


FIG. 2. ^7Li chemical shift spectra for crystalline alloys. The dots correspond to the measurements of Key *et al.* [7] and the solid lines to the present nearest-neighbors model. Vertical lines indicate the contributions of bonded and isolated Si.

there is an intermediate coexistence between bonded and isolated Si atoms. Finally, isolated Si atoms prevail at high lithium concentrations.

There is a better agreement between the model and experiment at high Li concentrations. At low Li concentrations, the experiment shows an extra contribution to the spectrum at 6 ppm, which is attributed to isolated Si atoms due to an inhomogeneous electrochemical lithiation [7], not present in the simulated lithiated structures. These simulations correspond to structures in thermodynamic equilibrium and do not take into account the processes that may occur in an inhomogeneous lithiation of the electrode, where highly lithiated regions exist at low overall lithium concentrations.

A different perspective on the study of local atomic structure was provided by Li *et al.* [12]. They used gamma rays to measure the ^{119}Sn Mössbauer spectra (MB) of amorphous $\text{Li}_x\text{Si}_{1-y}\text{Sn}_y$, for $0 < x < 3.5$ and small values of y [12]. Given the low concentration of tin, the authors assume that Sn atoms occupy the same sites of Si atoms in this material, making it equivalent to the result of an amorphous Si lithiation [20]. The MB signal consists of two peaks that almost completely overlap at the extreme cases of low or high lithium concentration, but are clearly separated for the intermediate cases. The separation distance, Δ , is expected to be sensitive to the local environment of Sn atoms. Δ reaches a maximum value around 1.2 mm/s at $x \sim 1$ and decreases for lower and higher concentrations, see triangles in Figure 4. The authors suggest that the maximum value of Δ is obtained when Sn atoms (and by analogy Si atoms) are surrounded by an equimolar mixture of Si and Li, and then decreases when some of the two atom types predominate. In order to make a quantitative statement in terms of this idea,

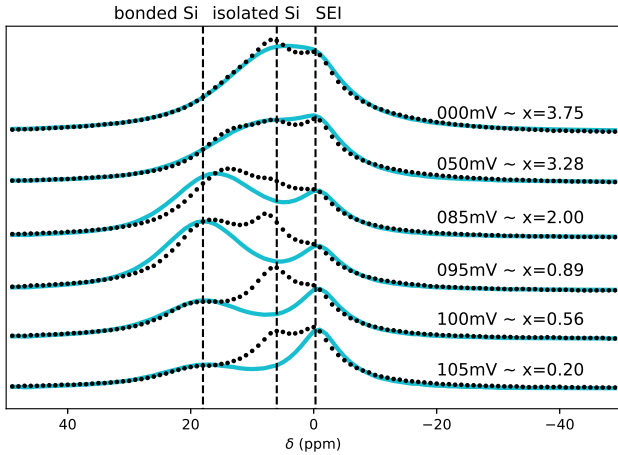


FIG. 3. ${}^7\text{Li}$ chemical shift spectra for amorphous structures. The dots correspond to the measurements of Key *et al.*[7]. The results of the present model are represented with solid lines and a SEI contribution is added for comparison. The vertical lines indicate the contributions of SEI and bonded or isolated Si atoms.

let us define the concentration of Li atoms, say C_{Li} and the concentration of Si atoms, say C_{Si} in terms of the number of Li atoms in the formula Li_xSi :

$$C_{Li} = \frac{x}{1+x} \quad ; \quad C_{Si} = 1 - C_{Li} \quad (3)$$

Now, since we find from the experimental results in Figure 4 that Δ tends to a constant value at small and large x values, we propose for Δ the following ansatz:

$$\Delta = a \min\{C_{Li}, C_{Si}\} + b \quad (4)$$

By tuning the a and b coefficients, it is possible to see (Figure 4) that this simple dependence yields the qualitative experimental trend (pink line). However, the definition given in equation 3 depends on the average of Li content of the alloy, while MB senses the local environment. We can seek a better agreement if we calculate the local concentration of Li and Si atoms by considering the nearest-neighbors of each Si atom for each of the amorphous alloys, as obtained from the averages of the simulations. If we replace into equation 4 the C_{Li} and C_{Si} values obtained from the simulations in this way, we get the cyan dots of Figure 4, showing an improved agreement with experiment.

We can summarize the results obtained herein by stating that we have used a recently developed DFTB model to generate the configuration of amorphous Li-Si alloys of different Li contents, covering the usual experimental range. These configurations lead to pair distribution functions that are in excellent agreement with experimental results. When the same configurations are used to predict NMR and Mössbauer spectra at different alloy

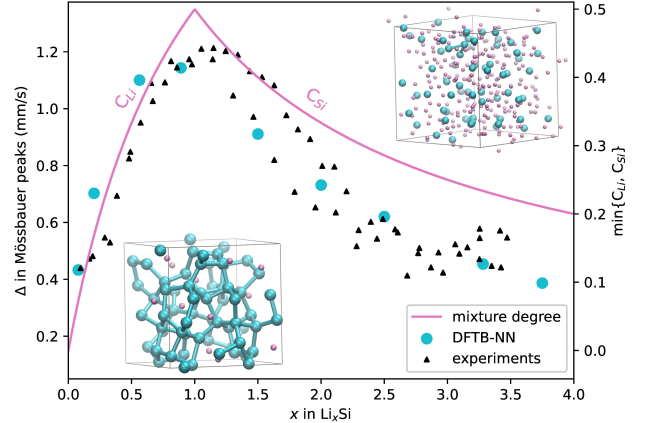


FIG. 4. Shift between the two peaks in the Mössbauer effect spectra. The triangles pointing up correspond to two measurements from Li *et al.* [12] (left axis), the solid line is the prediction of equation 4, using average concentrations of Li and Si atoms. The cyan circles are the prediction given by equation 4, with C_{Li} , C_{Si} calculated from the nearest-neighbors concentration (right axis).

compositions, also a very good agreement is found with experiment. The present results encourage to use this new DFTB to predict other properties of Li-Si alloys, a promising system in the field of Li-ion battery materials.

This work used computational resources from CCAD-UNC, which is part of SNCAD-MinCyT, Argentina. F.F. thanks his PhD fellowship from CONICET. We acknowledge financial support from CONICET (28720210100623CO, 28720210101190CO, 1220200101189CO, PUE/2017), the Agencia Nacional de Promoción Científica y Tecnológica (FONCyT 2020-SERIEA-02139, 2020-SERIEA-03689) and SECyT of the Universidad Nacional de Córdoba.

* apaz@unc.edu.ar

- [1] L. D. Harvey, *Global warming* (Routledge, 2018).
- [2] M. Obrovac and L. Christensen, Structural changes in silicon anodes during lithium insertion/extraction, *Electrochemical and Solid State Letters* **7**, A93 (2004).
- [3] D. Liu, Z. Shadike, R. Lin, K. Qian, H. Li, K. Li, S. Wang, Q. Yu, M. Liu, S. Ganapathy, *et al.*, Review of recent development of in situ/operando characterization techniques for lithium battery research, *Advanced Materials* **31**, 1806620 (2019).
- [4] B. Key, M. Morcrette, J.-M. Tarascon, and C. P. Grey, Pair distribution function analysis and solid state nmr studies of silicon electrodes for lithium ion batteries: understanding the (de) lithiation mechanisms, *Journal of the American Chemical Society* **133**, 503 (2011).
- [5] K. Pan, F. Zou, M. Canova, Y. Zhu, and J.-H. Kim, Systematic electrochemical characterizations of si and io

- anodes for high-capacity li-ion batteries, *Journal of Power Sources* **413**, 20 (2019).
- [6] N. Ding, J. Xu, Y. Yao, G. Wegner, X. Fang, C. Chen, and I. Lieberwirth, Determination of the diffusion coefficient of lithium ions in nano-si, *Solid State Ionics* **180**, 222 (2009).
- [7] B. Key, R. Bhattacharyya, M. Morcrette, V. Seznec, J.-M. Tarascon, and C. P. Grey, Real-time nmr investigations of structural changes in silicon electrodes for lithium-ion batteries, *Journal of the American Chemical Society* **131**, 9239 (2009).
- [8] M. B. Oviedo, F. Fernandez, M. Otero, E. Leiva, and S. A. Paz, Density functional tight-binding model for lithium-silicon alloys., (2022).
- [9] K. Laaziri, S. Kycia, S. Roorda, M. Chicoine, J. L. Robertson, J. Wang, and S. C. Moss, High Resolution Radial Distribution Function of Pure Amorphous Silicon, *Phys. Rev. Lett.* **82**, 3460 (1999).
- [10] T. K.-J. Köster, E. Salager, A. J. Morris, B. Key, V. Seznec, M. Morcrette, C. J. Pickard, and C. P. Grey, Resolving the different silicon clusters in li₁₂si₇ by 29si and 6, 7li solid-state nmr spectroscopy, *Angewandte Chemie International Edition* **50**, 12591 (2011).
- [11] K. Ogata, E. Salager, C. Kerr, A. Fraser, C. Ducati, A. J. Morris, S. Hofmann, and C. P. Grey, Revealing lithium-silicide phase transformations in nano-structured silicon-based lithium ion batteries via in situ nmr spectroscopy, *Nature communications* **5**, 3217 (2014).
- [12] J. Li, A. Smith, R. Sanderson, T. Hatchard, R. Dunlap, and J. Dahn, In situ 119sn mössbauer effect study of the reaction of lithium with si using a sn probe, *Journal of The Electrochemical Society* **156**, A283 (2009).
- [13] X. Wang, S. Tan, X.-Q. Yang, and E. Hu, Pair distribution function analysis: Fundamentals and application to battery materials, *Chinese Physics B* **29**, 028802 (2020).
- [14] V. Chevrier and J. R. Dahn, First principles model of amorphous silicon lithiation, *Journal of the Electrochemical Society* **156**, A454 (2009).
- [15] H. J. Berendsen, J. v. Postma, W. F. Van Gunsteren, A. DiNola, and J. R. Haak, Molecular dynamics with coupling to an external bath, *The Journal of chemical physics* **81**, 3684 (1984).
- [16] B. Hourahine, B. Aradi, V. Blum, F. Bonafé, A. Buccheri, C. Camacho, C. Cevallos, M. Deshayé, T. Dumitrică, A. Dominguez, *et al.*, Dftb+, a software package for efficient approximate density functional theory based atomistic simulations, *The Journal of chemical physics* **152**, 124101 (2020).
- [17] S. J. Billinge, The rise of the x-ray atomic pair distribution function method: a series of fortunate events, *Philosophical Transactions of the Royal Society A* **377**, 20180413 (2019).
- [18] J. Higinbotham and I. Marshall, Nmr lineshapes and line-shape fitting procedures, (2001).
- [19] A. Jain, S. P. Ong, G. Hautier, W. Chen, W. D. Richards, S. Dacek, S. Cholia, D. Gunter, D. Skinner, G. Ceder, *et al.*, Commentary: The materials project: A materials genome approach to accelerating materials innovation, *APL materials* **1**, 011002 (2013).
- [20] T. Hatchard, M. Obrovac, and J. Dahn, A comparison of the reactions of the s₁si, siag, and s₂si binary systems with l₃i, *Journal of The Electrochemical Society* **153**, A282 (2005).

SUPPLEMENTAL MATERIAL

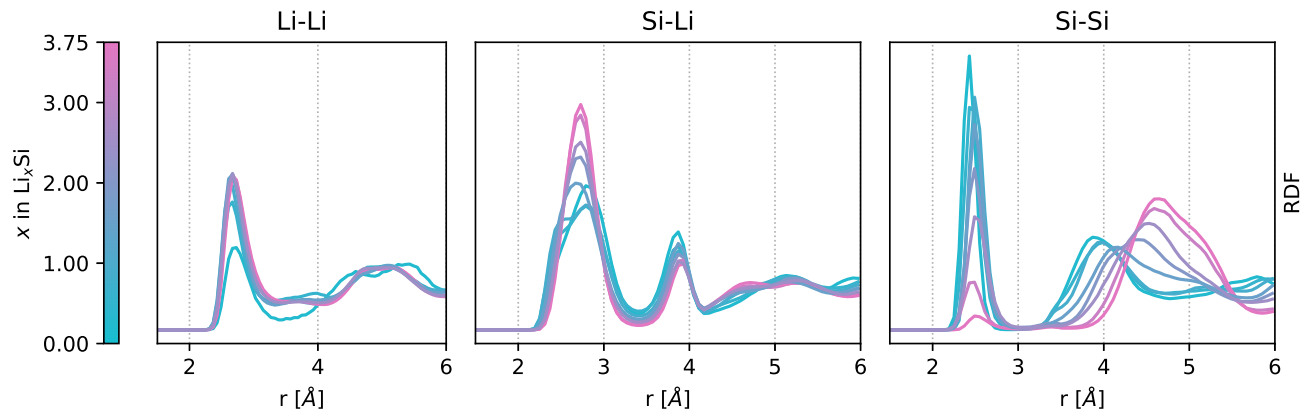


FIG. S1. Partial RDF for LiLi, SiLi and SiSi for all Li concentrations considered. The colour of the curve changes from cyan (Si predominance) to pink (Li predominance).

The $G(r)$ of the lithiated Si structure has the contributions of each structure S in $\{c\text{-Si}, c\text{-Li}_{15}\text{Si}_4, a\text{-Si}, a\text{-Li}_{15}\text{Si}_4\}$ multiplied by a factor w_S that were adjusted to minimize the mean squared error and are summarized in Table I,

$$G(r) = \sum_S w_S \cdot G_S(r), \quad (\text{S1})$$

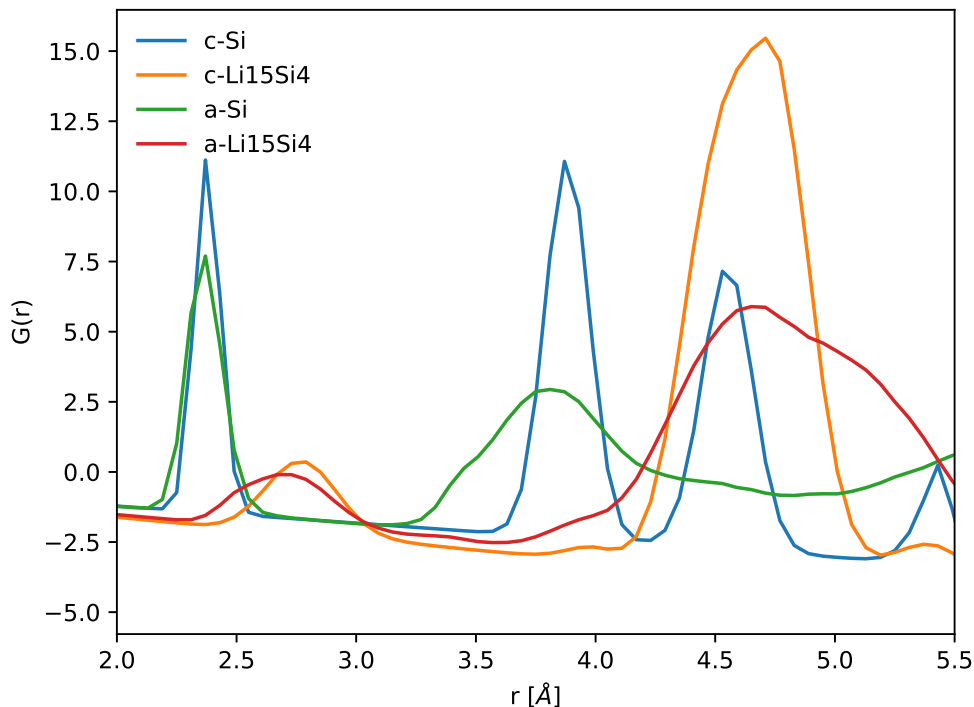


FIG. S2. Pair distribution functions $G(r)$ of crystalline and amorphous structures used to compute the curves shown in Figure 1 of the manuscript.

TABLE I. Weight factor of each contribution (c-Si, c-Li₁₅Si₄, a-Si and a-Li₁₅Si₄) to the pair distribution function $G(r)$ of lithiated Si, shown in Figure 1 of the main text. The percentage represented by each weight is shown in parentheses. $G(r)$ was calculated using equation S1.

Fitting	c-Si	c-Li ₁₅ Si ₄	a-Si	a-Li ₁₅ Si ₄
crystalline	0.03358 (30.15%)	0.077784 (69.85%)	–	–
DFTB amorphous	0.0 (0.0%)	0.036422 (9.78%)	0.187971 (50.48%)	0.147955 (39.74%)

where each $G_S(r)$ is shown in Figure S2 and can be calculated using that

$$G_S(r) = 4\pi r \rho_{0,S} [g_S(r) - 1], \quad (\text{S2})$$

where $\rho_{0,S}$ is the atomic number density and $g_S(r)$ is the atomic radial distribution function of the structure S and can be computed by considering the scattering factor b_i of each atom i in the following way [17]

$$g_S(r) = \frac{1}{4\pi\rho_0 r^2 N} \sum_i \sum_{j \neq i} \frac{b_i b_j}{\langle b \rangle^2} \delta(r - r_{ij}), \quad (\text{S3})$$

where $\langle b \rangle$ is the average scattering factor, N the total number of atoms and r_{ij} is the distance between atoms i and j . The scattering factors for Li and Si atoms are 3 and 14, respectively. This gives us that the Si-Si RDF contributes in a 82%, the Si-Li RDF in a 16% and the Li-Li RDF in a 3%.

In Figure S3 a simplified 2D unit cell with periodic boundary conditions is presented to explain the nearest-neighbor model that predicts the results of NMR chemical shift spectra for LiSi systems. Each Li atom contributes with a Voigt peak, as stated in the main text, where it centers depends on the type of Si atoms (bonded or isolated) that are in its first coordination shell. The cut-off radius for the first coordination shell can be seen in the Si-Si RDF in Figure S1, it is seen that the same is maintained for all concentrations at 3.4Å. For example, for Li atom 1 we have

$$\delta_1 = \frac{18\text{ppm} + 6\text{ppm}}{2} = 12\text{ppm},$$

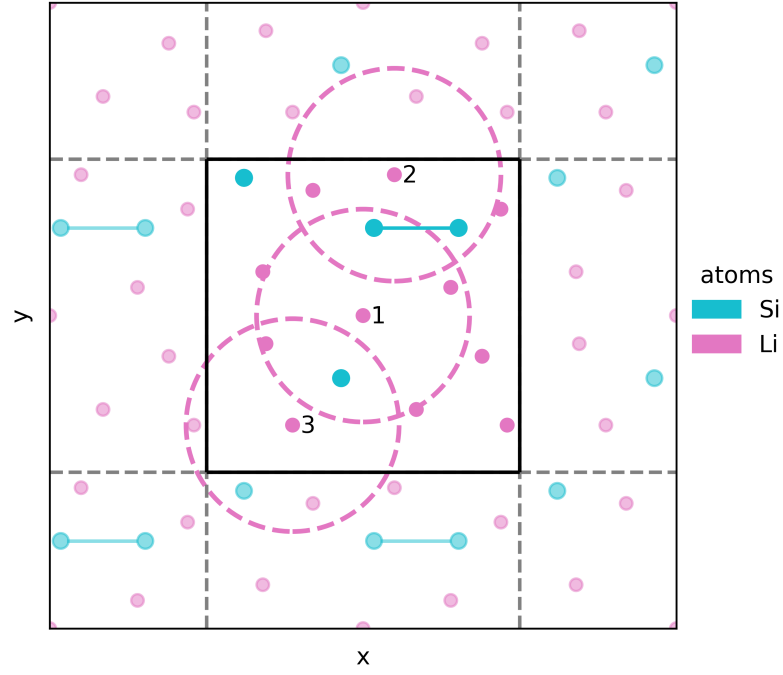


FIG. S3. Diagram to explain the nearest-neighbor model that predicts the results of NMR experiments on LiSi systems.

where the 18 ppm and 6 ppm come from the bonded and the isolated Si atom, respectively. In the same way, Li atom 2 has a

$$\delta_2 = \frac{18\text{ppm} + 18\text{ppm}}{2} = 18\text{ppm},$$

and Li atom 3 a

$$\delta_3 = \frac{6\text{ppm} + 6\text{ppm}}{2} = 6\text{ppm}.$$

Then, the intensity of the spectra generated from these three atoms has is a sum of contributions

$$I = V_1(12\text{ppm}) + V_2(18\text{ppm}) + V_3(6\text{ppm}) + \dots,$$

and so on as we consider the rest of the Li atoms in the structure.
